

Physical Properties of $[A_6Cl][Fe_{24}Se_{26}]$ ($A = K, Rb$) with Self-Similar Structure *

Shaohua Wang(王少华), Qiangwei Yin(殷蔷薇), Hechang Lei(雷和畅)**

Department of Physics and Beijing Key Laboratory of Opto-electronic Functional Materials & Micro-nano Devices, Renmin University of China, Beijing 100872

(Received 13 September 2019)

We have successfully synthesized two novel compounds $[A_6Cl][Fe_{24}Se_{26}]$ ($A = K, Rb$). The key structural units of them are FeSe octamers, consisting of edge-shared $FeSe_4$ tetrahedra. Two kinds of FeSe octamer layers with different connection configurations stack along the c axis, forming a three-dimensional (3D) $TiAl_3$ -type structure. Interestingly, the 3D structural topology of these octamers in one unit cell is similar to the local atomic arrangement of themselves, i.e., self-similarity in structure. Physical property characterizations indicate that both the compounds exhibit insulating antiferromagnetism with Neel temperatures $T_N \sim 110$ K and 75 K for $[K_6Cl][Fe_{24}Se_{26}]$ and $[Rb_6Cl][Fe_{24}Se_{26}]$.

PACS: 74.50.+r, 75.20.Ck, 75.30.-m, 75.30.Cr

DOI: 10.1088/0256-307X/37/1/017401

Iron-based materials have been explored extensively because they exhibit intriguing physical properties, such as high-temperature superconductivity and low-dimensional magnetism.^[1–8] Most iron-based superconductors, varying from $LnFeAsO$ ($Ln = La, Ce, Pr, Sm$),^[2] $AeFe_2As_2$ ($Ae = Ba, Sr, Ca$),^[3–5] $AFeAs$ ($A = Li, Na$),^[9,10] to $FeSe$,^[11] have the common key structural ingredient of a two-dimensional (2D) square Fe lattice, consisting of edge-shared FeX_4 ($X = pnictogens$ and $chalcogens$) tetrahedra.^[9,11–14] In contrast, low-dimensional antiferromagnetism emerges in $AFeCh_2$ ($A = Na, K, Cs$; $Ch = S, Se$) with one-dimensional (1D) Fe chains^[6] and $BaFe_2Ch_3$ with 1D Fe ladders.^[7,8,15] By decreasing the dimensionality of the Fe lattice, these compounds show insulating behaviors under ambient pressure due to the bandwidth narrowing and enhanced correlation effect. Surprisingly, $BaFe_2Ch_3$ demonstrates superconductivity under high pressure, challenging the known superconducting theory for iron-based superconductors.^[16–19] On the other hand, ternary compound $CaFe_4As_3$ with a 3D framework of Fe lattice displays long-range antiferromagnetic (AFM) order at low temperature together with non-Fermi-liquid behavior at zero-field and enhanced electron-electron correlation.^[20] However, the compounds with 3D Fe lattice are still scarce and their physical properties are also barely studied in $FeCh$ -based materials.^[21]

Recently, an FeSe-based compound $[Cs_6Cl][Fe_{24}Se_{26}]$ with a 3D framework composed of $FeSe_4$ tetrahedra was reported. It exhibits insulating behavior with long-range AFM transition at $T_N \sim 221$ K.^[22] Motivated by that study, in the present work we find two novel compounds $[A_6Cl][Fe_{24}Se_{26}]$ ($A = K, Rb$), which are isostructural to $[Cs_6Cl][Fe_{24}Se_{26}]$. AFM ordering states are observed below 110 K and 75 K for

both the insulating materials.

Polycrystal samples of $[A_6Cl][Fe_{24}Se_{26}]$ ($A = K, Rb$) are grown by solid state reaction method. A_2Se , as the precursor in the following step, was synthesized using A lumps (99.8%, sigma) and Se shots (99.999%, aladdin) with the molar ratio of 2 : 1. The A_2Se , ACl (98%, aladdin), Fe (98%, alfa), and Se (99.9%, aladdin) powders were mixed with the molar ratio of 2.5 : 1 : 24 : 23.5 and ground adequately in an agate mortar. The well-ground mixture was pressed into pellets and loaded into an alumina crucible. All the above-mentioned procedures were carried out in the glove box with the O_2 and H_2O contents under 0.1 ppm. Then, the crucible was sealed in a quartz tube. The ampule was heated up to 773 K for 12 h and kept at this temperature for 60 h, then cooled to room temperature for 6 h. X-ray diffraction (XRD) patterns were collected using a Bruker D8 x-ray diffractometer with $Cu K_\alpha$ radiation ($\lambda = 1.5418 \text{ \AA}$) at room temperature. The lattice parameters were obtained by Rietveld refinement using the TOPAS4 software.^[23] Magnetization measurements were performed in a Quantum Design magnetic property measurement system (MPMS3). Resistivity measurements were performed in Quantum Design physical property measurement system (PPMS-14).

Figure 1 presents the powder XRD patterns of $[K_6Cl][Fe_{24}Se_{26}]$ and $[Rb_6Cl][Fe_{24}Se_{26}]$, respectively. Both the patterns can be well fitted with the previously reported structure of $[Cs_6Cl][Fe_{24}Se_{26}]$ (space group $I4/mmm$).^[22] The refined lattice parameters are $a = 10.834(2) \text{ \AA}$, $c = 21.624(5) \text{ \AA}$ for $[K_6Cl][Fe_{24}Se_{26}]$ and $a = 10.946(9) \text{ \AA}$, $c = 21.85(4) \text{ \AA}$ for $[Rb_6Cl][Fe_{24}Se_{26}]$ and details of the refinement are listed in Table 1. When compared with $[Cs_6Cl][Fe_{24}Se_{26}]$ ($a = 11.0991 \text{ \AA}$, $c = 22.143 \text{ \AA}$), the trend of lattice parameters in these compounds can be

*Supported by the National Key R&D Program of China under Grant No. 2016YFA0300504, the National Natural Science Foundation of China (Nos. 11574394, 11774423, 11822412), the Fundamental Research Funds for the Central Universities, and the Research Funds of Renmin University of China (RUC) (15XNLLQ07, 18XNLLG14, 19XNLLG17).

**Corresponding author. Email: hlei@ruc.edu.cn

© 2020 Chinese Physical Society and IOP Publishing Ltd

ascribed to the gradually increased ionic radius from K to Cs.

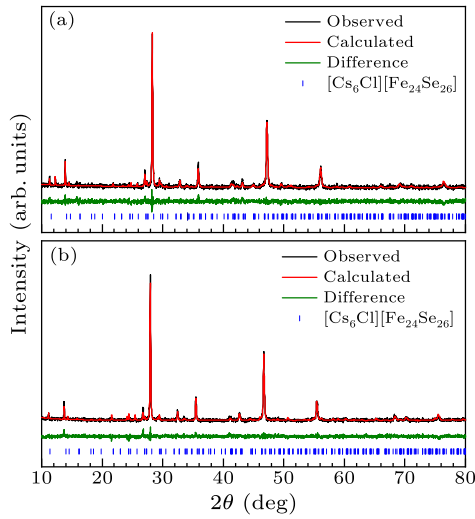


Fig. 1. (a) and (b) Powder XRD patterns and Rietveld refinements of $[\text{K}_6\text{Cl}][\text{Fe}_{24}\text{Se}_{26}]$ and $[\text{Rb}_6\text{Cl}][\text{Fe}_{24}\text{Se}_{26}]$ using the structure of $[\text{Cs}_6\text{Cl}][\text{Fe}_{24}\text{Se}_{26}]$.

Table 1. Refinement details of $[\text{K}_6\text{Cl}][\text{Fe}_{24}\text{Se}_{26}]$ and $[\text{Rb}_6\text{Cl}][\text{Fe}_{24}\text{Se}_{26}]$ using XRD data at room temperature.

$[\text{K}_6\text{Cl}][\text{Fe}_{24}\text{Se}_{26}]$				
Unit Cell (\AA)		$a = 10.834(2) \quad c = 21.624(5)$		
Atom	Site	x	y	z
K1	$4e$	0	0	0.1669(5)
K2	$8i$	0.3239(7)	0	0
Cl1	$2a$	0	0	0
Fe1	$16m$	0.375(4)	0.375(4)	0.0641(7)
Fe2	$32o$	0.3730(1)	0.1311(2)	0.1877(6)
Se1	$8g$	0.5	0	0.1132(2)
Se2	$8j$	0.5	0.245(8)	0
Se3	$4e$	0	0	0.6346(7)
Se4	$16n$	0	0.7556(9)	0.7475(6)
Se5	$16m$	0.239(9)	0.239(9)	0.1179(2)
$R_{\text{exp}} = 1.97\%, R_{\text{wp}} = 3.31\%$				
$[\text{Rb}_6\text{Cl}][\text{Fe}_{24}\text{Se}_{26}]$				
Unit Cell (\AA)		$a = 10.946(9) \quad c = 21.85(4)$		
Rb1	$4e$	0	0	0.1609(1)
Rb2	$8i$	0.2965(4)	0	0
Cl1	$2a$	0	0	0
Fe1	$16m$	0.375(4)	0.375(4)	0.0650(6)
Fe2	$32o$	0.3802(6)	0.1329(8)	0.1875(6)
Se1	$8g$	0.5	0	0.1153(4)
Se2	$8j$	0.5	0.2477(8)	0
Se3	$4e$	0	0	0.6395(6)
Se4	$16n$	0	0.7528(1)	0.7472(7)
Se5	$16m$	0.239(9)	0.239(9)	0.1169(9)
$R_{\text{exp}} = 5.48\%, R_{\text{wp}} = 6.19\%$				

The structure of this family, taking $[\text{Rb}_6\text{Cl}][\text{Fe}_{24}\text{Se}_{26}]$ as an example, is shown in Fig. 2(a). It mainly consists of Rb_6Cl octahedra and octamers formed by edge sharing FeSe_4 tetrahedra. Rb_6Cl octahedra are located at the position of vertexes and body center in a unit cell. There are two kinds of octamers of FeSe_4 tetrahedra (labelled in different colors) stacking along the c axis alternatively. The structure of $[\text{A}_6\text{Cl}][\text{Fe}_{24}\text{Se}_{26}]$ is closely related to the TiAl_3 -type structure depicted in Fig. 2(b). The Ti

atoms are replaced by the A_6Cl octahedra and two different Al sites now are occupied by two kinds of octamers of FeSe_4 tetrahedra.^[22] As shown in Figs. 2(c) and 2(d), Fe1 octamers (green) locating at the edges of a unit cell do not connect each other in the plane, but Fe2 octamers (orange) form a two-dimensional layer via corner sharing. In addition, the Fe octamers in different layers are also connected by corner sharing via Se5 atoms.

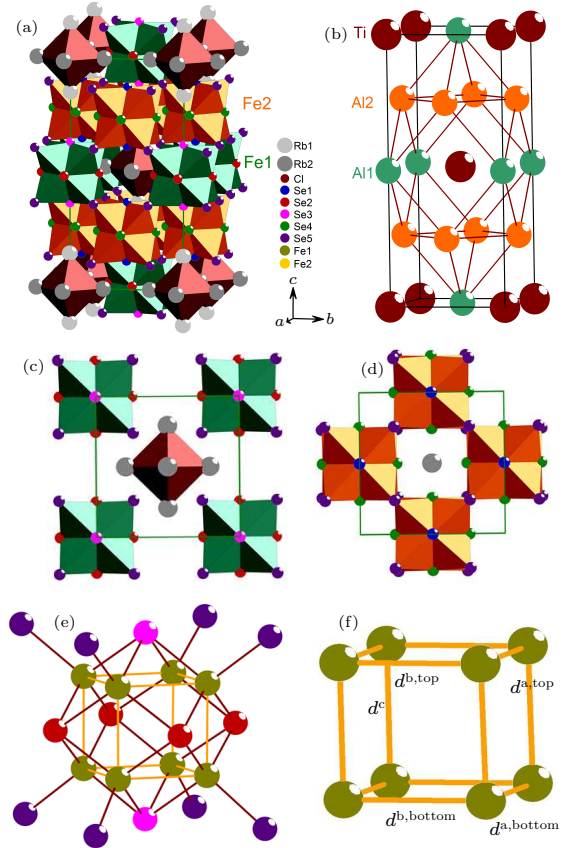


Fig. 2. (a) The structure of $[\text{Rb}_6\text{Cl}][\text{Fe}_{24}\text{Se}_{26}]$ as an example of this type of compound, (b) TiAl_3 -type structure, (c) and (d) the arrangement of Fe1 and Fe2 octamers in the ab plane, (e) an enlarged view of one octamer, (f) definition of $d_{\text{Fe-Fe}}$ along different axes in one octamer.

Table 2. Fe-Fe distances $d_{\text{Fe-Fe}}$ of the two types of octamers along different axes for $[\text{K}_6\text{Cl}][\text{Fe}_{24}\text{Se}_{26}]$ and $[\text{Cs}_6\text{Cl}][\text{Fe}_{24}\text{Se}_{26}]$.

Distance	$[\text{K}_6\text{Cl}][\text{Fe}_{24}\text{Se}_{26}]$		$[\text{Rb}_6\text{Cl}][\text{Fe}_{24}\text{Se}_{26}]$	
	Fe1-Fe1	Fe2-Fe2	Fe1-Fe1	Fe2-Fe2
$d_{\text{Fe-Fe}}^{a,\text{top}}$	2.6999(8) \AA	2.841(2) \AA	2.7277(5) \AA	2.6214(5) \AA
$d_{\text{Fe-Fe}}^{b,\text{top}}$	2.6999(8) \AA	2.7516(8) \AA	2.7277(5) \AA	2.9111(9) \AA
$d_{\text{Fe-Fe}}^{a,\text{bottom}}$	2.6999(8) \AA	2.7516(8) \AA	2.7277(5) \AA	2.9111(9) \AA
$d_{\text{Fe-Fe}}^{b,\text{bottom}}$	2.6999(8) \AA	2.841(2) \AA	2.7277(5) \AA	2.6214(5) \AA
$d_{\text{Fe-Fe}}^c$	2.7754(4) \AA	2.6926(8) \AA	2.8436(4) \AA	2.7367(3) \AA

Figure 2(e) shows the isolated structure of an FeSe_4 octamer. This subunit is built up of double layers of four edge-shared FeSe tetrahedra with sharing common Se^{2-} anions in the middle. Similar subunit has also been observed in ACu_4Se_3 ^[24] and recently reported CuAs -based materials $\text{Re}_2\text{Cu}_5\text{As}_3\text{O}_2$ with Cu_5As_3 cage.^[25] Interestingly, this subunit is

analogous to the arrangement of Al atoms in a TiAl_3 structure. Thus, $[\text{A}_6\text{Cl}][\text{Fe}_{24}\text{Se}_{26}]$ compounds have the self-similarity in structures, i.e., Se and Fe in one FeSe octamer are equivalent to the Fe1 and Fe2 octamers. On the other hand, the Fe–Fe distances $d_{\text{Fe–Fe}}$ of the two types of octamers (defined in Fig. 2(f)) for both the compounds are listed in Table 2. It can be seen that the distances of Fe2–Fe2 are slightly different in the ab plane compared to the equivalent values for Fe1–Fe1. Moreover, the distance of Fe2–Fe2 along the c axis is compressed when compared to the in-plane values, but this is inverse for Fe1–Fe1. This may be related to the stretching effect of A_6Cl octahedra for Fe1 octamers. The values of $d_{\text{Fe–Fe}}$ in $[\text{A}_6\text{Cl}][\text{Fe}_{24}\text{Se}_{26}]$ are much larger than that in FeSe ($d_{\text{Fe–Fe}} = 2.6689 \text{ \AA}$) and slightly larger than the intralayer $d_{\text{Fe–Fe}}$ of spin ladder compounds BaFe_2S_3 (2.698 \AA) and BaFe_2Se_3 (2.707 \AA).^[7,8]

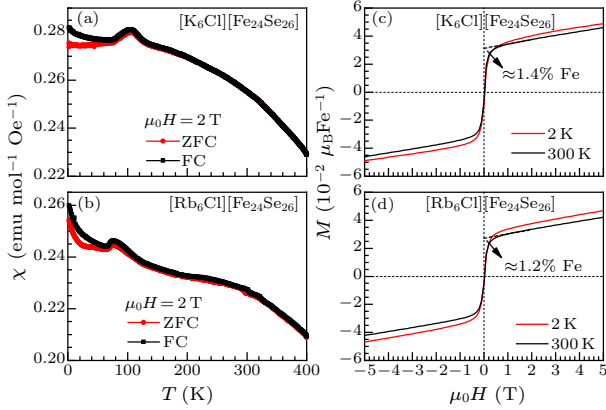


Fig. 3. (a) and (b) Temperature dependence of magnetic susceptibility measured at $\mu_0 H = 2 \text{ T}$ for $[\text{K}_6\text{Cl}][\text{Fe}_{24}\text{Se}_{26}]$ and $[\text{Rb}_6\text{Cl}][\text{Fe}_{24}\text{Se}_{26}]$. (c) and (d) Isothermal magnetization loops at $T = 2 \text{ K}$ and 300 K for $[\text{K}_6\text{Cl}][\text{Fe}_{24}\text{Se}_{26}]$ and $[\text{Rb}_6\text{Cl}][\text{Fe}_{24}\text{Se}_{26}]$.

Figures 3(a) and 3(b) present the temperature dependence of magnetic susceptibility $\chi(T)$ for $[\text{K}_6\text{Cl}][\text{Fe}_{24}\text{Se}_{26}]$ and $[\text{Rb}_6\text{Cl}][\text{Fe}_{24}\text{Se}_{26}]$ polycrystals under magnetic field $\mu_0 H = 2 \text{ T}$ with zero-field-cooling (ZFC) and field-cooling (FC) modes from 2 K to 400 K . The concave shapes of $\chi(T)$ curves for both compounds indicate a deviation from the Curie–Weiss behavior at the high temperatures, implying the possible existence of short-range magnetic interaction. With lowering temperature, a small peak appears at about 110 K and 75 K for $[\text{K}_6\text{Cl}][\text{Fe}_{24}\text{Se}_{26}]$ and $[\text{Rb}_6\text{Cl}][\text{Fe}_{24}\text{Se}_{26}]$, respectively, suggesting a formation of long-range AFM order. The weak difference between ZFC and FC $\chi(T)$ curves for both the compounds below the AFM transition temperature (T_N) implies that the magnetic glassy state may be negligible. The field dependence of magnetization $M(\mu_0 H)$ at 2 K and 300 K are shown in Figs. 3(c) and 3(d) for $[\text{K}_6\text{Cl}][\text{Fe}_{24}\text{Se}_{26}]$ and $[\text{Rb}_6\text{Cl}][\text{Fe}_{24}\text{Se}_{26}]$, respectively. It can be seen that both $M(\mu_0 H)$ curves below and above T_N exhibit ferromagnetic behaviors, similar to those in $[\text{Cs}_6\text{Cl}][\text{Fe}_{24}\text{Se}_{26}]$.^[22] This is ascribed to the

unreacted Fe impurities. The estimated content of Fe second phase at 300 K is about 1% for both the compounds (Figs. 3(c) and 3(d)), close to that of $[\text{Cs}_6\text{Cl}][\text{Fe}_{24}\text{Se}_{26}]$.^[22]

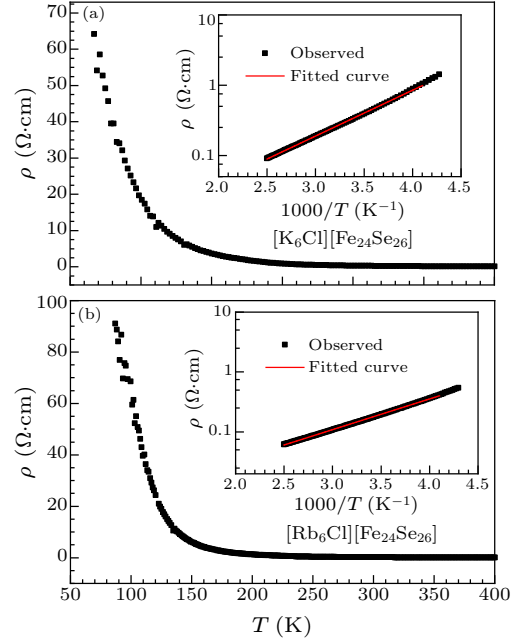


Fig. 4. Temperature dependence of resistivity $\rho(T)$ for (a) $[\text{K}_6\text{Cl}][\text{Fe}_{24}\text{Se}_{26}]$ and (b) $[\text{Rb}_6\text{Cl}][\text{Fe}_{24}\text{Se}_{26}]$. Insets: the fitting results of $\rho(T)$ in the high temperature region using thermal activation model. The red lines are the fitted curves.

Temperature dependence of resistivity $\rho(T)$ for $[\text{K}_6\text{Cl}][\text{Fe}_{24}\text{Se}_{26}]$ and $[\text{Rb}_6\text{Cl}][\text{Fe}_{24}\text{Se}_{26}]$ polycrystals at zero field are plotted in Fig. 4. The values of $\rho(T)$ for $[\text{K}_6\text{Cl}][\text{Fe}_{24}\text{Se}_{26}]$ and $[\text{Rb}_6\text{Cl}][\text{Fe}_{24}\text{Se}_{26}]$ at 300 K are about 0.30 \Omega cm and 0.15 \Omega cm , respectively, which are larger than that in $[\text{Cs}_6\text{Cl}][\text{Fe}_{24}\text{Se}_{26}]$ but comparable with the quasi-1D spin ladder compound BaFe_2S_3 .^[7,22] Both the compounds show insulating behaviors in the whole measuring temperature range. The temperature dependence of $\rho(T)$ at high temperature can be well fitted using the thermal activation model $\rho = \rho_0 \exp(E_a/k_B T)$, where ρ_0 is a prefactor, E_a is the thermal activated energy, and k_B is the Boltzmann constant (insets of Fig. 4). The fitted E_a are 129 meV and 102 meV for $[\text{K}_6\text{Cl}][\text{Fe}_{24}\text{Se}_{26}]$ and $[\text{Rb}_6\text{Cl}][\text{Fe}_{24}\text{Se}_{26}]$, which are much larger than the evaluated value in $[\text{Cs}_6\text{Cl}][\text{Fe}_{24}\text{Se}_{26}]$ ($\sim 7.6 \text{ meV}$).^[22]

In summary, we have synthesized two novel compounds $[\text{A}_6\text{Cl}][\text{Fe}_{24}\text{Se}_{26}]$ ($A = \text{K}, \text{Rb}$), isostructural to $[\text{Cs}_6\text{Cl}][\text{Fe}_{24}\text{Se}_{26}]$. The key structural ingredient is the self-similar 3D framework of FeSe octamers. The magnetization measurements indicate that $[\text{K}_6\text{Cl}][\text{Fe}_{24}\text{Se}_{26}]$ and $[\text{Rb}_6\text{Cl}][\text{Fe}_{24}\text{Se}_{26}]$ show AFM transitions at $T_N \sim 110 \text{ K}$ and 75 K , respectively, accompanying with the possible short-range magnetic interaction at room temperature. Both the compounds exhibit insulating behaviors and the fitted E_a values using the thermal activation model are

129 meV and 102 meV, which are much larger than the previously reported data for $[\text{Cs}_6\text{Cl}][\text{Fe}_{24}\text{Se}_{26}]$.

References

- [1] Kamihara Y, Watanabe T, Hirano M and Hosono H 2008 *J. Am. Chem. Soc.* **130** 3296
- [2] Karpinski J, Zhigadlo N D, Katrych S, Bukowski Z, Moll P, Weyeneth S, Keller H, Puzniak R, Tortello M, Daghero D, Gonnelli R, Maggio-Aprile I, Fasano Y, Fischer O, Rogacki K and Batlogg B 2009 *Physica C* **469** 370
- [3] Sefat A S, Jin R Y, McGuire M A, Sales B C, Singh D J and Mandrus D 2008 *Phys. Rev. Lett.* **101** 117004
- [4] Torikachvili M S, Bud'ko S L, Ni N and Canfield P C 2008 *Phys. Rev. Lett.* **101** 057006
- [5] Yan J Q, Kreyszig A, Nandi S, Ni N, Bud'ko S L, Kracher A, McQueeney R J, McCallum R W, Lograsso T A, Goldman A I and Canfield P C 2008 *Phys. Rev. B* **78** 024516
- [6] Seidov Z, Krug von Nidda H A, Tsurkan V, Filippova I G, Gunther A, Gavrilova T P, Vagizov F G, Kiiamov A G, Tagirov L R and Loidl A 2016 *Phys. Rev. B* **94** 134414
- [7] Gönen Z S, Fournier P, Smolyaninova V, Greene R, Araujo-Moreira F M and Eichhorn B 2000 *Chem. Mater.* **12** 3331
- [8] Lei H C, Ryu H, Frenkel A I and Petrovic C 2011 *Phys. Rev. B* **84** 214511
- [9] Wang X C, Liu Q Q, Lv Y X, Gao W B, Yang L X, Yu R C, Li F Y and Jin C Q 2008 *Solid State Commun.* **148** 538
- [10] Chu C W, Chen F, Gooch M, Guloy A M, Lorenz B, Lv B, Sasmal K, Tang Z J, Tapp J H and Xue Y Y 2009 *Physica C* **469** 326
- [11] Hsu F C, Luo J Y, Yeh K W, Chen T K, Huang T W, Wu P M, Lee Y C, Huang Y L, Chu Y Y, Yan D C and Wu M K 2008 *Proc. Natl. Acad. Sci. USA* **105** 14262
- [12] Rotter M, Tegel M and Johrendt D 2008 *Phys. Rev. Lett.* **101** 107006
- [13] Parker D R, Pitcher M J, Baker P J, Franke I, Lancaster T, Blundell S J and Clarke S J 2009 *Chem. Commun.* **2009** 2189
- [14] Lu X F, Wang N Z, Wu H, Wu Y P, Zhao D, Zeng X Z, Luo X G, Wu T, Bao W, Zhang G H, Huang F Q, Huang Q Z and Chen X H 2015 *Nat. Mater.* **14** 325
- [15] Caron J M, Neilson J R, Miller D C, Llobet A and McQueeney T M 2011 *Phys. Rev. B* **84** 180409(R)
- [16] Takahashi H, Sugimoto A, Nambu Y, Yamauchi T, Hirata Y, Kawakami T, Avdeev M, Matsubayashi K, Du F, Kawashima C, Soeda H, Nakano S, Uwatoko Y, Ueda Y, Sato T J and Ohgushi K 2015 *Nat. Mater.* **14** 1008
- [17] Yamauchi T, Hirata Y, Ueda Y and Ohgushi K 2015 *Phys. Rev. Lett.* **115** 246402
- [18] Ying J J, Lei H C, Petrovic C, Xiao Y M, Struzhkin V V 2017 *Phys. Rev. B* **95** 241109(R)
- [19] Mazin I I 2010 *Nature* **464** 183
- [20] Karki A B, McCandless G T, Stadler S, Xiong Y M, Li J, Chan J Y and Jin R 2011 *Phys. Rev. B* **84** 054412
- [21] Tani B S 1977 *Am. Mineral.* **62** 819
- [22] Valldor M, Bohme B, Prots Y, Borrmann H, Adler P, Schnelle W, Watier Y, Kuo C Y, Pi T W, Hu Z W, Felser C and Tjeng L H 2016 *Chem. Eur. J.* **22** 4626
- [23] TOPAVersion 4.2 S 2009 Bruker AXS, Karlsruhe, Germany
- [24] Sturza M, Bugaris D E, Malliakas C D, Han F, Chung D Y and Kanatzidis M G 2016 *Inorg. Chem.* **55** 4884
- [25] Chen X, Guo J G, Gong C S, Cheng E, Le C C, Liu N, Ying T P, Zhang Q H, Hu J P, Li S Y and Chen X L 2019 *iScience* **14** 171